Investigation of short range ordering in polymers: 3. Studies of low molecular weight alkanes and molten polyethylene

G. W. Longman
ICI Corporate Laboratory, P. O. Box 11, The Heath, Runcorn, Cheshire, UK
G. D. Wignall
Oak Ridge National Laboratories, Oak Ridge, Tennessee 37830, USA
R. P. Sheldon
School of Polymer Science, University of Bradford, Bradford, UK
(Received 16 November 1978; revised 9 March 1979)

Radial distribution function methods have been used to compare the short range ordering (*SRO*) in molten polyethylene, with that in a number of n-alkanes. The *SRO* as monitored by the number and amplitude of intermolecular peaks increases with the number of carbon atoms in the alkane to C_{16}, which has a similar degree of *SRO* to hexatriacontane (C_{36}). The observed ordering decreases with increasing temperature, but the higher alkanes show less temperature dependence than the lower alkanes. For none of the measured systems do the intermolecular correlations persist over distances greater than ~20 Å, and the *SRO* observed in molten polyethylene is similar to that for the lower alkanes. The data does not support suggestions in the literature that the *SRO* should increase progressively with chain length to give a substantially parallel arrangement of chain segments in molten polyethylene over regions 50–100 Å in size.

INTRODUCTION

There has been considerable debate over the degree of short range order (*SRO*) in amorphous polymers, and the extent to which it is enhanced by marked asymmetry in the shape of the polymer molecules[1]. In the case of molten polyethylene, Ovchinnikov and coworkers[2,3] have claimed to have detected regular intermolecular spacings indicative of chains packed approximately parallel over distances of 50–100 Å. This experimental data was challenged by Voigt–Martin and Mijlhoff[4] and Longman *et al.*[5], who observed a degree of *SRO* only slightly greater than the low levels found in glassy amorphous polymers.

There are also conflicting views on the type of order present in liquid n-alkanes, and calorimetric studies[6,7] have been interpreted in terms of a correlation of molecular orientation (*CMO*) between neighbouring segments of alkane molecules. This evidence was supported by data on light depolarization[8], which was also consistent with the existence of a *CMO* which increased with chain length up to C_{16}. Boyer has pointed out[9] that it is difficult to understand why these two different techniques show that the *SRO* is still increasing up to C_{16}, whereas neutron scattering[10,11] and X-ray measurements[5] failed to detect any long-range ordering in liquid polyethylene. On the other hand, Flory has suggested[12] that *SRO* may exist in polymers but not to a greater degree than for low molecular weight liquids.

Diffraction methods can provide further information on the degree of short range ordering and radial distribution function (*RDF*) methods have been widely used to characterize amorphous and semicrystalline materials[2–4,13,14]. The *RDF* from a polyatomic material gives to a good approximation a summation over the different interatomic distances in the system, and hence reflects the tendency of atoms to correlate at given distances depending on the type and degree of order. *RDF* measurements cannot in general determine the type of order or distinguish the ordering processes involved in the system. For example both an increased *CMO* and increased perfection of lateral intermolecular spacings can lead to an increased tendency of atoms to correlate at typical intermolecular distances (~5 Å), and both mechanisms would increase the number and amplitude of the intermolecular peaks in the *RDF*. However, the method can be used to distinguish intermolecular and intramolecular correlations[13,14] and can usefully be employed to monitor changes in the degree of intermolecular correlations in the sample thus comparing different levels of *SRO*. Furthermore, *RDF* data can be used to test the various models which have been proposed for liquid and amorphous systems, both with respect to the average amplitude, and range of the correlations observed. We have therefore used *RDF* methods to explore the differing viewpoints on the structure of alkanes, by measuring molten polyethylene and a series of n-alkanes with the same techniques.

Earlier studies of molten polyethylene by electron diffraction[2,3] have shown the need for very careful data correction procedures, which have been discussed in detail by Voigt–Martin and Mijlhoff[4]. Similar *RDF* curves may be derived from X-ray diffraction data and some results for molten polyethylene have been given previously[5,15]. This paper describes the application of these techniques, using X-ray diffraction, to some low molecular weight n-alkanes.

EXPERIMENTAL

The experimental methods used have been described in detail previously[14]. Measurements were performed on a Picker

0032–3861/79/091063–08$02.00

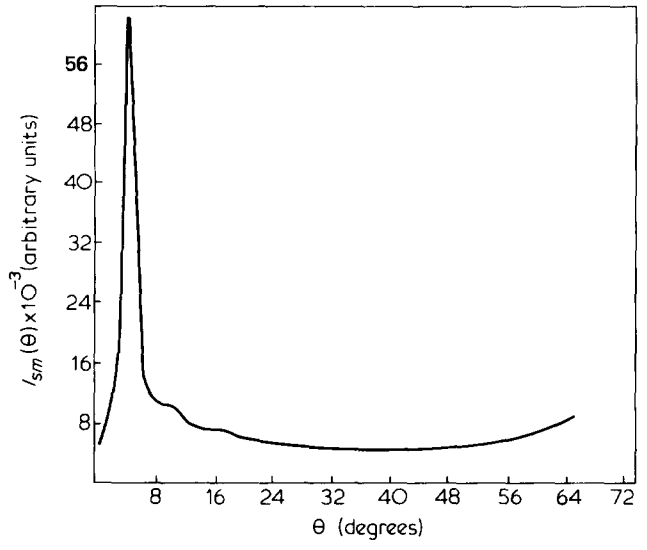

Figure 1 Intensity, $I_{sm}(\theta)$ vs. θ for hexane

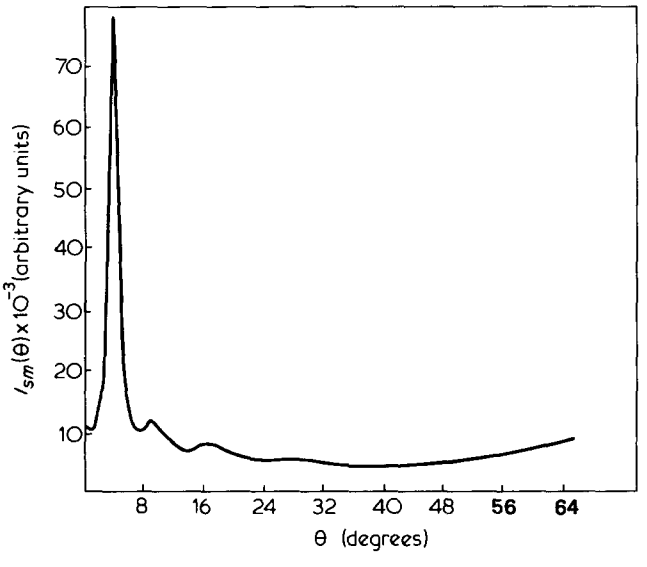

Figure 2 Intensity, $I_{sm}(\theta)$ vs. θ for molten polyethylene

Automatic 4 Circle Diffractometer within the range $0.11 < S < 16.1$ Å^{-1} where $S = (4\pi/\lambda)\sin\theta$; 2θ is the scatter angle and $\lambda = 0.71$ Å is the wavelength of the incident molybdenum Kα radiation. The samples were held in a cell approximately 1 mm thick with thin 'Melinex' film windows (~18 μm thick). The sample temperature for the lowest molecular weight alkanes was room temperature (~23°C), and for the higher melting samples and polyethylene the sample was heated by two heaters, wound on mica formers and placed either side of the sample, the required temperature control to within ±2°C being by means of a chromel/alumel thermocouple.

The scattered data were corrected for incoherent scattering, absorption in the sample and 'Melinex' cell walls, double scattering and polarization of the scattered beam. The methods for performing these corrections, and for choosing the collimation limits, monochromatizing the incident beam etc. are described in ref 14. The data were normalized using the dispersion corrected form factors of Berghuis[16] and Stewart[17], and incoherent scattering factors of Keating and Vineyard[18]. The resulting *RDF*, $H(r)$, was calculated from

$$H(r) = \frac{1}{2\pi^2\bar{\rho}r}\int_{S_{min}}^{S_{max}} Si(S)\sin rS\,dS$$

where $\bar{\rho}$ is the mean atomic density (atoms/unit volume) of the sample, $S_{min} = 0.11$ Å^{-1} and $S_{max} = 16.1$ Å^{-1}, and $i(S)$ is the interference function derived from the normalized intensity data.

RESULTS

Intensity data were collected on a fixed count basis, i.e. the time for a fixed count (10 000) on each of the two balanced filters (Zr/Yt) was recorded and subsequently converted to a plot of count rate for a given time interval. *Figures 1* and *2* show smoothed plots of $I_{sm}(\theta) = I^{\beta} - I^{\alpha}$ corrected for incident intensity drift by repeated checks on the intensity at a fixed angle throughout the run. *Figure 1* shows the measured intensity for n-hexane (23°C) and *Figure 2* that for for molten polyethylene (160°C); the two patterns are typical of those for disordered materials. Similar patterns were obtained for octane (C_8H_{18}), hexadecane ($C_{16}H_{34}$) at 23°C and hexatriacontane ($C_{36}H_{74}$) at 77°C. The radial distribution function, $H(r)$, for hexane and molten polyethylene are given in *Figures 3* and *4*. *Figure 5* shows a plot of $H(r)$ for solid n-hexatriacontane. Each of the peaks at small values

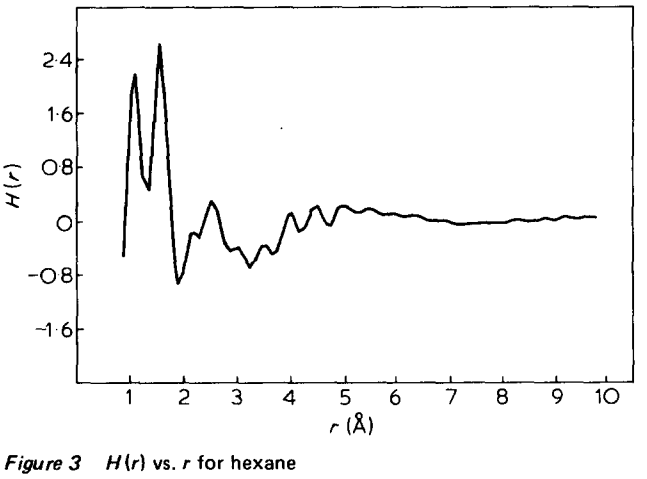

Figure 3 $H(r)$ vs. r for hexane

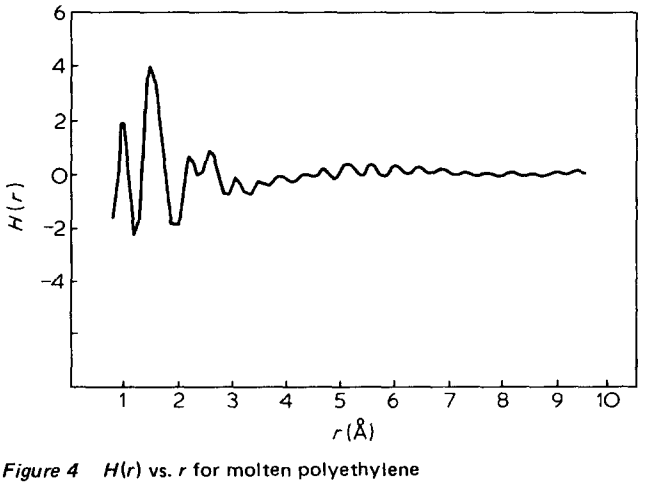

Figure 4 $H(r)$ vs. r for molten polyethylene

for r arises from one or more interatomic distances within the structural repeat unit of the sample. The plots show marked similarities, especially for $r < 6$ Å as do plots of $H(r)$ for the other samples examined. This is not unexpected as the repeat unit ($-CH_2-$) is essentially the same for all the samples. A full list of the types of interatomic distances occurring within a few repeat units are given in *Tables 1* and *2* for the all *trans* and *tgtgtg* configurations. At values of $r > 5$ Å intermolecular atomic distances play an increasingly important role, but the peaks decay rapidly in the plots of $H(r)$ in this region. *SRO* arising from intermolecular atomic distances is better seen by plotting the second moment of the *RDF*, $4\pi r^2 \bar{\rho} H(r)$ over an extended range of r. As the ordinate is extremely sensitive to small errors at high values of r in view of the r^2 weighting, an exponential damping factor $e^{-\alpha^2 s^2}$ (where $\alpha = 0.11$) is applied to the interference function before transformation. This value was chosen to reduce most of the high frequency (0.4 Å) oscillation (due most probably to residual truncation errors), whilst leaving the low frequency (~5 Å) structural features unaffected.

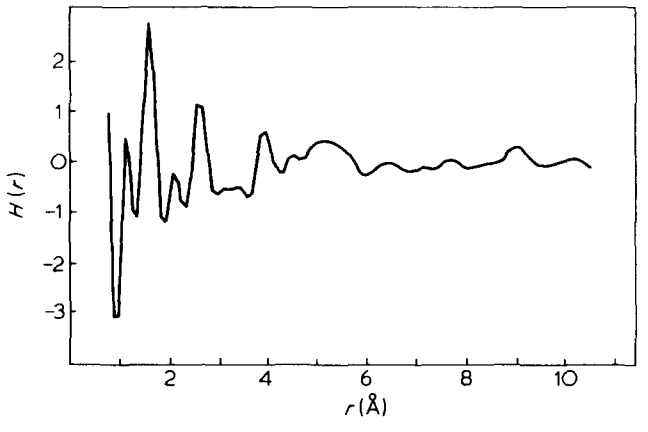

Figure 5 $H(r)$ vs. r for solid hexatriacontane at room temperature (23°C)

Plots of $4\pi r^2 \bar{\rho} H(r)$ for hexane, octane and hexadecane at room temperature, and hexadecane (60°C), hexatriacontane (77° and 110°C) and molten polyethylene (160°C) at elevated temperatures are given in *Figures 6–12*, respectively. Characteristic features of these plots are the broad oscillations of frequency ~5 Å. These peaks arise largely from intermolecular spacings[13,19] and as the *SRO* in a sample increases, the number of intermolecular peaks resolved, together with their amplitude, increases. This may clearly be seen by comparing the plots of molten and solid hexatriacontane (*Figures 10* and *13*, respectively). The latter sample was prepared by quenching the molten alkane in acetone/drikold mixture to obtain a microcrystalline sample, although the degree of ordering present is still much greater than that normally encountered in samples subjected to *RDF* analysis. The *RDF* of this crystalline sample shows resolvable peaks out to ~70 Å, with an approximate period ~4 Å, which arise from the greatly increased intermolecular order in the sample. There are several processes contributing to the increased order, including an increased *CMO* as the molecules become more parallel, and increased perfection in lateral spacings as the material crystallizes. The *RDF* gives only an averaged correlation of atoms at given interatomic spacings and cannot resolve the contribution of each process to the ordering. However, it can be used to give an overall indication of the degree of *SRO* in a material, and has been shown to be sensitive to small changes in the *SRO*[13,14,19].

Table 1 Interatomic distances for *trans* configuration

Type	Description	r_{ij}	A_{ij}	*RDF* peak*
C–H	Carbon–hydrogen bond, C_1-H_1 etc.	1.13	300.2	1.15
C–C	Carbon–carbon bond, C_1-C_2 etc.	1.53	517.4	
H–H	Methylene hydrogen interatomic distance, H_4-H_5 etc. + methyl hydrogen interatomic distances	1.75	21.5	1.57
C–H	Carbon–hydrogen on next carbon, C_1-H_4 etc.	2.15	210.4	
C–H	Methyl hydrogen to next carbon, C_2-H_1 etc.	2.25	50.3	2.20
C–C	Carbon–next but one carbon, C_1-C_3 etc.	2.54	267.1	
H–H	Hydrogen to hydrogen on next but one carbon, H_4-H_8 etc.	2.54	32.1	
H–H	Hydrogen to hydrogen on next carbon, H_4-H_6 etc.	–	–	2.57
H–H	Methyl hydrogen to hydrogen on next carbon, H_1-H_4 etc.	2.65	4.8	
C–H	Carbon to hydrogen on next but one carbon, C_1-H_6 etc.	2.75	137.0	
H–H	Hydrogen to diagonal hydrogen on next but one carbon H_4-H_9 etc.	3.05	8.2	
H–H	Hydrogen to diagonal hydrogen on next carbon, H_4-H_7 etc.	3.15	18.0	3.10
C–H	Methyl hydrogen to next but two carbon, C_3-H_1 etc.	3.55	10.6	3.45
H–H	Methyl hydrogen to hydrogen on next but two carbon H_1-H_6 etc.	3.85	3.3	
C–C	Carbon to next but two carbon, C_1-C_4 etc.	3.95	143.2	3.96
C–H	Carbon to hydrogen on next but two carbon, C_1-H_8 etc.	4.25	88.7	
H–H	Hydrogen–hydrogen on next but two carbon, H_4-H_{10} etc.	4.45	7.1	
C–H	Methyl hydrogen to next but three carbon, H_1-C_4 etc.	4.75	7.9	4.53
H–H	Hydrogen to diagonal hydrogen on next but two carbon, H_4-H_{11} etc.		6.6	
H–H	Methyl hydrogen to hydrogen on next but two carbon, H_1-H_8 etc.	4.95	2.5	
C–C	Carbon–next but three carbon, C_1-C_5 etc.	5.05	89.6	5.17
H–H	Methyl hydrogen–hydrogen on next but three carbon, H_2-H_{10} etc.		1.2	
H–H	Hydrogen–hydrogen on next but three carbon, H_4-H_{12} etc.	5.15	3.7	

* *RDF* peaks, solid hexatriacontane

DISCUSSION

In general, the peaks observed in the *RDF* plot for a polymer are attributable either to intramolecular atomic distances arising from the polymer repeat units, or to intermolecular atomic distances determined by the short range ordering or packing of the polymer chains. The intensity or area under the *RDF* resulting from an i–j bond at r_{ij} has been defined[14] as:

$$A_{ij} = \sum_{uc} \sum_{i} \frac{N_{ij}}{r_{ij}} Z_i Z_j \frac{\pi}{2}$$

where Z_i and Z_j are the atomic numbers of the ith and jth

Table 2 Interatomic distances for *tgtgtg* configuration

Type	Description	r_{ij}	A_{ij}	*RDF* peak*
C–H	Carbon–hydrogen bond, C_1–H_1 etc.	1.13	300.2	1.10
C–C	Carbon–carbon bond, C_1–C_2 etc.	1.53	517.4	
H–H	Methylene and methyl hydrogen interatomic distances H_1–H_2 etc.	1.75	21.5	1.54
H–H	Hydrogen–hydrogen at ends of *gauche*, H_6–H_{12}, etc.	2.05	4.6	
C–H	Carbon–hydrogen on next carbon, C_1–H_4 etc.	2.15	210.4	2.15
C–H	Carbon–methyl hydrogen on next carbon, C_2–H_1 etc.	2.25	50.3	
H–H	Hydrogen to hydrogen on next carbon, H_4–H_6 etc.	2.45	3.8	
C–C	Carbon to next but one carbon, C_1–C_3 etc.	2.54	267.1	2.64
H–H	Hydrogen to hydrogen on next but one carbon, H_6–H_8 etc.	2.54	4.9	
H–H	Methyl hydrogen to hydrogen on next atom, H_1–H_4 etc.	2.55	9.9	
H–H	Hydrogen to hydrogen on next diagonal carbon, H_4–H_7 etc.	2.55	7.4	
H–H	Hydrogen to diagonal hydrogen on next but one carbon, H_4–H_9 etc.	2.55	4.9	
C–H	Carbon to hydrogen on next but two carbon, C_3–H_{12} etc.	2.65	28.5	
H–H	Methyl hydrogen to hydrogen on next but one carbon, H_3–H_6 etc.	2.65	2.4	
C–H	Carbon to hydrogen on next but one carbon, C_2–H_8 etc.	2.75	68.5	
C–H	Carbon to hydrogen on next but one carbon, C_2–H_8 etc.	2.85	66.1	
H–H	Hydrogen to diagonal hydrogen on next but two carbon, H_7–H_{12} etc.	2.95	6.4	
C–C	Carbon to next but two carbon across *gauche*, C_1–C_4 etc.	3.05	111.2	3.12
H–H	Hydrogen to diagonal hydrogen on next carbon, H_6–H_9 etc.	3.05	6.2	
H–H	Methyl hydrogen to hydrogen on next carbon, H_3–H_4 etc.	3.15	4.0	
H–H	Hydrogen to hydrogen on next carbon, H_4–H_6 etc.	3.15	5.0	
H–H	Methyl hydrogen to hydrogen on next but one carbon	3.25	1.9	
C–H	Carbon to hydrogen on next but two carbon, C_1–H_9 etc.	3.35	22.5	
C–H	Carbon to methyl hydrogen C_4–H_3 etc.	3.45	10.9	3.55
C–H	Carbon to hydrogen on next but one carbon across *gauche*, C_1–H_7 etc.	3.55	42.5	
H–H	Methyl hydrogen to hydrogen on next but two carbon, H_1–H_8 etc.	3.65	1.7	
H–H	Hydrogen to hydrogen on next but one carbon, H_5–H_9 etc.	3.75	3.3	
H–H	Methyl hydrogen to hydrogen on next but one carbon, H_2–H_7 etc.	3.85	4.9	
H–H	Hydrogen to diagonal hydrogen on next but one carbon, H_5–H_8 etc.	3.85	3.3	3.94
C–C	Carbon to next but two carbon, C_2–C_5 etc.	3.95	57.3	
C–H	Methyl hydrogen to next but 3 carbon, C_4–H_1 etc.	4.05	18.6	
C–H	Carbon to hydrogen on next 3 carbon, C_1–H_{12} etc.			
H–H	Hydrogen to hydrogen on next but two carbon, H_3–H_9 etc.	4.05	2.3	
C–H	Methyl hydrogen to next but four carbon, H_2–C_5 etc.	4.15	9.1	
C–H	Carbon to hydrogen on next but two carbon, C_2–H_{10} etc.	4.25	17.7	
H–H	Methyl hydrogen to hydrogen on next but four carbon, H_2–H_{13} etc.	4.25	5.9	
H–H	Methyl hydrogen to hydrogen on next but one carbon, H_1–H_7 etc.	4.35	1.4	4.35
C–C	Carbon to next but three carbon, C_1–C_5 etc.	4.45	101.7	
H–H	Hydrogen to hydrogen on next but two carbon H_4–H_{10} etc.	4.45	2.8	
C–H	Hydrogen to carbon on next but three carbon H_5–H_{12} etc.			
C–H	Carbon to hydrogen on next but four carbon, C_1–H_{12} etc.	4.55	24.9	
C–H	Carbon to hydrogen on next but three carbon, C_2–H_{13} etc.			
H–H	Methyl hydrogen to hydrogen on fourth carbon, H_2–H_{11}	4.55	1.4	
H–H	Methyl hydrogen to hydrogen on next but three carbon, H_4–H_{17} etc.	4.65	24.3	
C–H	Methyl hydrogen to hydrogen on next but four carbon, C_6–H_2 etc.	–	–	4.76
H–H	Methyl hydrogen to hydrogen on next but four carbon, H_2–H_{12} etc.	4.65	1.4	
C–H	Carbon to hydrogen on next but two carbon C_2–H_{11} etc.	4.75	15.9	
C–C	Carbon to next but four carbon, C_1–C_6 etc.	4.85	46.6	
H–H	Hydrogen to hydrogen on next but three carbon H_4–H_{12}	4.85	1.3	
H–H	Methyl hydrogen to hydrogen on next but three carbon H_2–H_{10} etc.	4.95	3.8	
H–H	Hydrogen to diagonal on next but two carbon, H_4–H_{11} etc.			
C–H	Carbon to hydrogen on next but three carbon C_1–H_{10} etc.	5.05	29.9	
H–H	Hydrogen to hydrogen on next but three carbon, H_4–H_{13} etc.	5.25	2.4	5.20
H–H	Methyl hydrogen to hydrogen on next but three carbon H_3–H_{10} etc.	5.35	2.4	

* RDF peaks for molten polyethylene

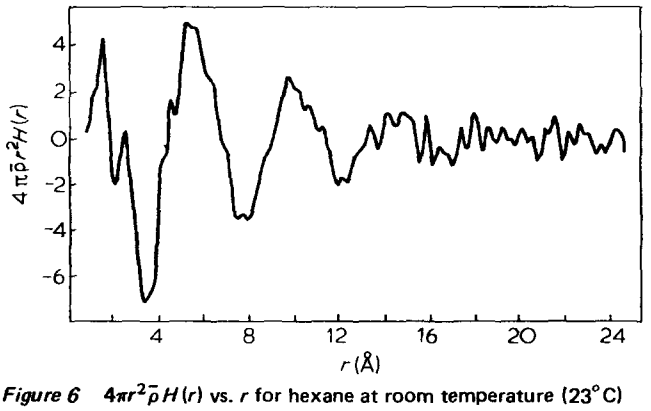

Figure 6 $4\pi r^2\bar{\rho}H(r)$ vs. r for hexane at room temperature (23°C)

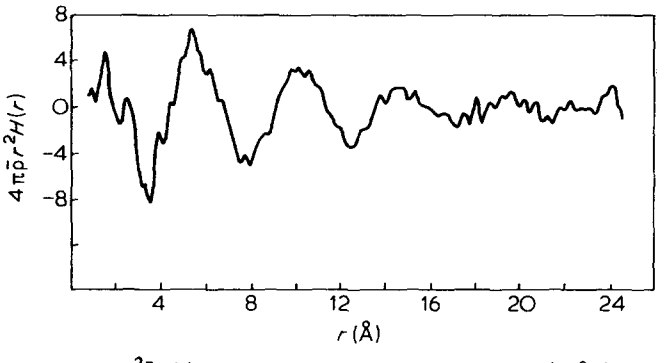

Figure 7 $4\pi r^2\bar{\rho}H(r)$ vs. r for octane at room temperature (23°C)

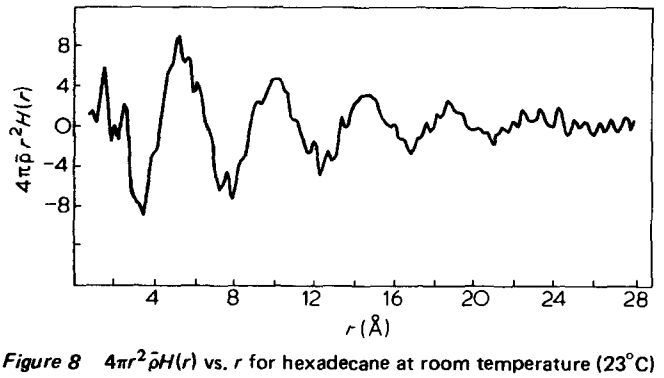

Figure 8 $4\pi r^2\bar{\rho}H(r)$ vs. r for hexadecane at room temperature (23°C)

atoms, r_{ij} is the interatomic distance, N_{ij} is the number of neighbours in the jth shell about the i atom and Σ_{uc} refers to a summation over a unit of composition, which is the polymer repeat unit (or a defined number of units). The intramolecular distances calculated for the *trans* configuration of an isolated octane molecule are given in *Table 1* together with the values of A_{ij}. Similar values for the *tgtgtg* conformation are given in *Table 2*, and a schematic diagram of the molecule is given in *Figure 12*. Histogram plots of the quantity A_{ij} for the two configurations are given in *Figures 13* and *14*. It is apparent that the interatomic distances of the immediately neighbouring carbon and hydrogen atoms do not vary with conformation so that the peaks at 1.13, 1.54, 2.2 and 2.5 Å remain unaltered. In the *tgtgtg* configuration there is an increase in relative intensity of the peaks at ~3.14 and ~4.4 Å, with a decrease in those at ~3.9 and ~5 Å. Peaks in the *RDF* at values of r ~5 Å and greater, will be increasingly dominated by intermolecular atomic distances arising from interactions with neighbouring chains, and these distances are clearly absent from the model calculations for the isolated octane molecule.

Comparing the experimentally derived plots of $H(r)$ for hexane and molten polyethylene with that for solid hexatriacontane, shows that the peaks at ~3.1 Å in the two liquid samples are both relatively stronger than that observed in the hexatriacontane, whereas the peaks at ~3.95 Å are weaker. These observations are consistent with the predicted increase in the number of *gauche* configurations occurring

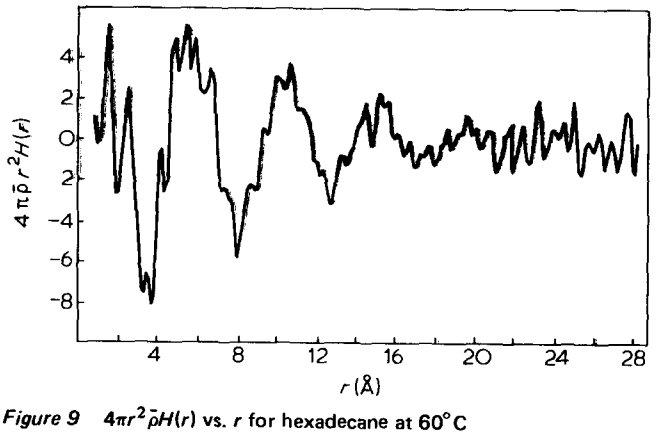

Figure 9 $4\pi r^2\bar{\rho}H(r)$ vs. r for hexadecane at 60°C

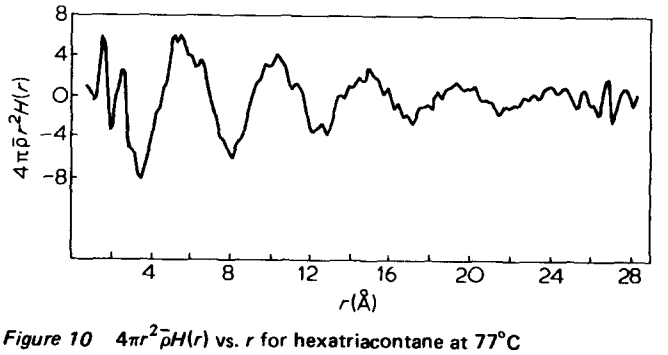

Figure 10 $4\pi r^2\bar{\rho}H(r)$ vs. r for hexatriacontane at 77°C

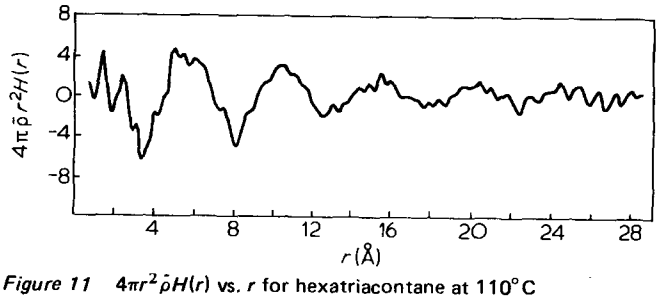

Figure 11 $4\pi r^2\bar{\rho}H(r)$ vs. r for hexatriacontane at 110°C

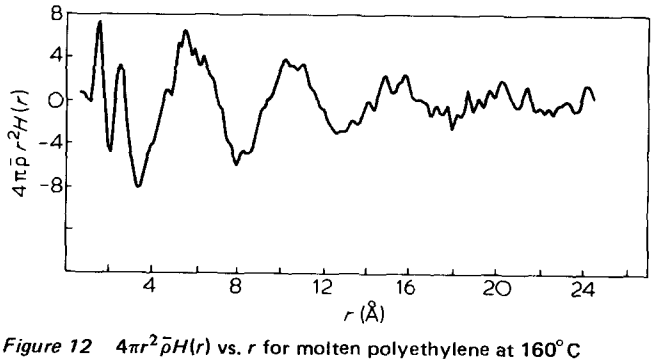

Figure 12 $4\pi r^2\bar{\rho}H(r)$ vs. r for molten polyethylene at 160°C

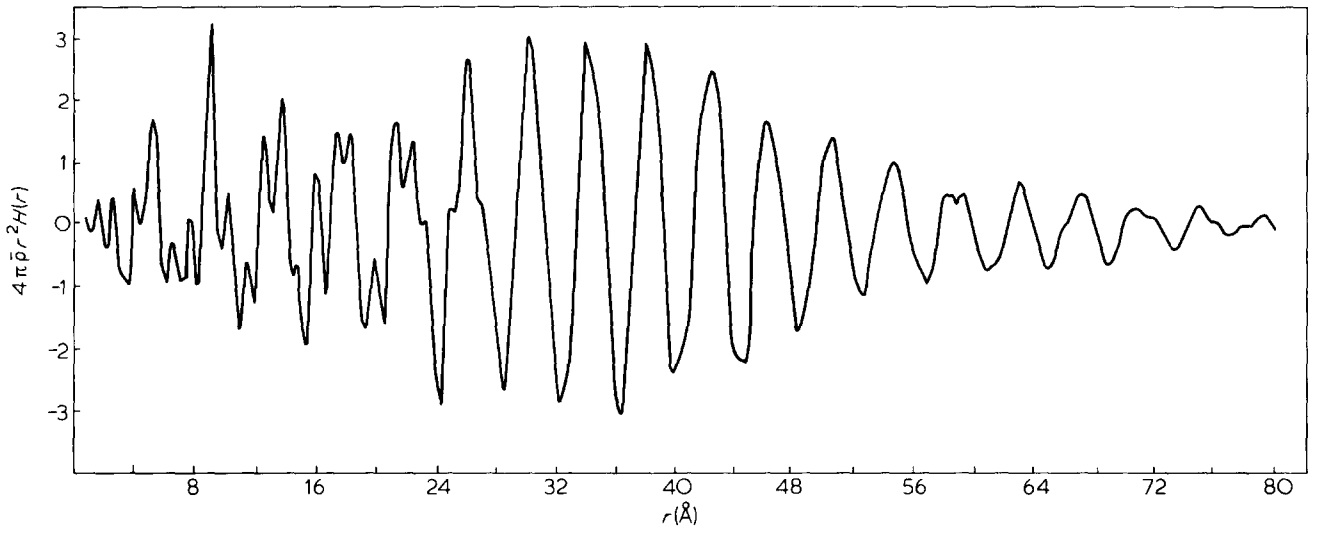

Figure 13 $4\pi r^2\bar{\rho}H(r)$ vs. r for solid hexatriacontane at room temperature (23°C)

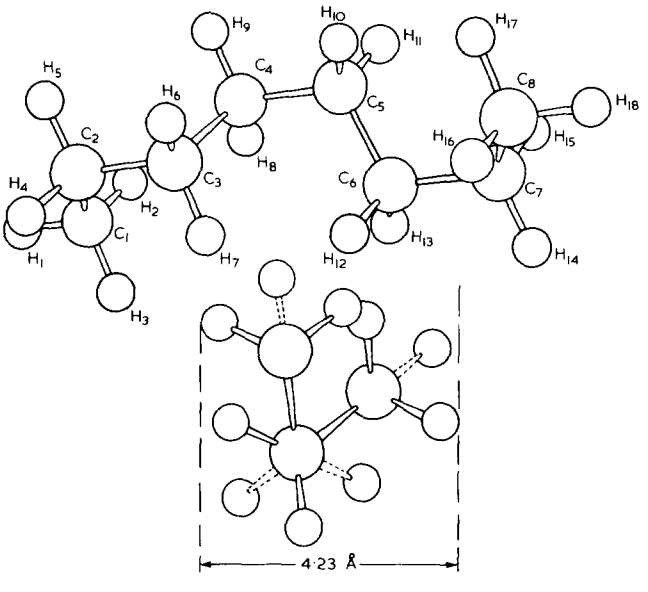

Figure 14 Schematic diagram of octane molecule, *tgtgtg* conformation

in the molten samples compared with the solid hexatriacontane, which is essentially in the all *trans* configuration. There is reasonable agreement at low r between the experimental curve (*Figure 5*) and the all *trans* model calculation (*Figure 13*). However, one would not expect close agreement for $r > 5$ Å, in view of the fact that the model calculations for an isolated molecule cannot give rise to intermolecular spacings.

Plots of the second moment of the *RDF* $4\pi r^2\bar{\rho}H(r)$ show the broad oscillations with a frequency of ~5 Å attributable to intermolecular ordering. The number of peaks resolved and hence the amount of short-range order, increases with the number of carbon atoms in the alkane up to C_{16} (hexadecane) at constant temperature. The observed ordering as monitored by the number and amplitude of intermolecular peaks in hexatriacontane just above the melting point (77°C) is similar to that for hexadecane at room temperature, and thus the degree of ordering does not increase with chain length after C_{16}.

The ordering decreases with increasing temperature and this effect is more marked for hexadecane than with hexatriacontane. This latter behaviour is similar to that observed in the temperature range 145°–317°C for molten polyethylene[20]. A possible explanation for this difference in temperature dependence is the nature of the observed ordering. Raising the temperature should decrease the ordering in all systems, but in the case of the lower alkanes an increase in the number of *gauche* configurations may have a more marked effect on the packing behaviour because of the small size and extreme mobility of the molecules. In the higher alkanes and molten polyethylene the disordering manifests itself as a decrease in the height of the peaks. The number of peaks resolved remains the same because only short segments of each molecule are involved in the intermolecular interaction, and increasing the thermal energy of the system (increasing temperature) may not greatly reduce this level of interaction.

The amount of intermolecular ordering resolved in molten polyethylene in this work is similar to that for octane at room temperature. The molecular weight of the polymer is several orders of magnitude greater than that of the higher alkanes investigated, and thus the intermolecular ordering does not increase in a corresponding manner, but is apparently less than that for the C_{16} and C_{36} alkanes. This could be due to the higher melting temperature of the molten polyethylene compared with the alkanes, but in view of the comparative insensitivity to change in temperature of the observed ordering in C_{36} and polyethylene remarked on earlier, this is probably not the case; on balance it seems more probable that there actually is inherently less ordering in the polymer.

The peak positions are given in *Table 3;* the intermolecular distances increasing with sample temperature, but remaining constant with varying molecular weight at any one temperature. The peak positions and relative intensities of the peaks are consistent with hexagonal packing of the molecules both in the liquid alkanes and molten polyethylene, as was previously shown by electron diffraction for the latter material[3]. It is also apparent that the peak positions for the solid hexatriacontane do not fit this pattern, as the values are not only different but the peaks show a 'doublet' effect due to the crystalline orthorhombic packing of this sample. The inter-

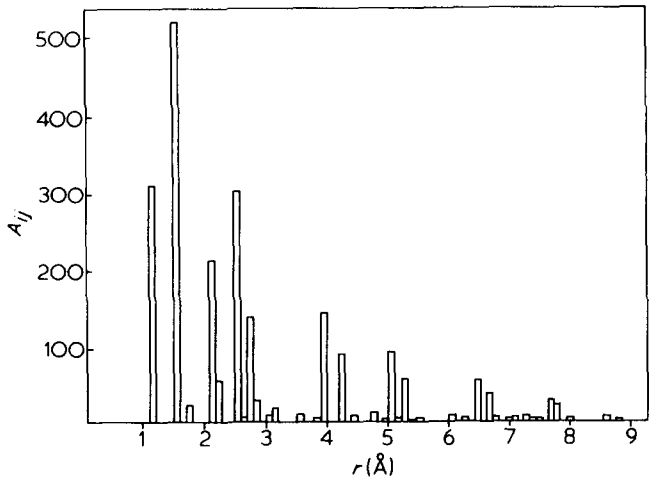

Figure 15 A_{ij} vs. r for *trans* configuration

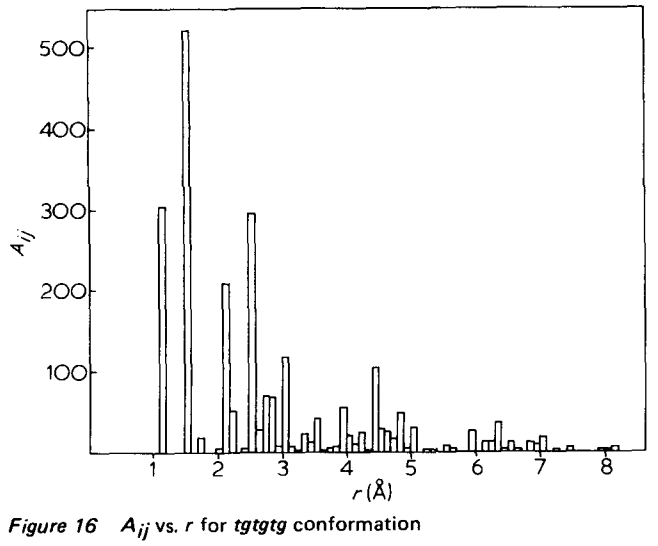

Figure 16 A_{ij} vs. r for *tgtgtg* conformation

molecular ordering in this sample is also considerably greater than that observed in the liquid samples. The ordering observed in molten polyethylene is similar to that for the lower liquid alkanes, but it is still greater than that resolved in some glassy amorphous polymers[11,14]. The existence of some nearest neighbour intermolecular peaks would be expected simply in terms of the geometrical packing of polymer chains with a diameter ~5 Å. As suggested previously[3], this may be enhanced in the case of polyethylene by the approximately cylindrical cross-section of the molecule, and the comparative invariance of the dimensions whether the carbon backbone is in the *trans* or *gauche* configuration.

Since the *RDF* gives only an average over the different interatomic spacings in the liquid, it is not possible to determine the type of ordering process involved from the *RDF* alone. A better understanding can therefore be obtained by considering the evidence from other techniques, and the extent to which the various models proposed for liquid alkanes and polyethylene are consistent with the *RDF* data. Results obtained from heat of mixing and light scattering studies[5–7] have suggested a *CMO* between neighbouring segments of alkane molecules. Recent depolarized Rayleigh and scattering studies[21] indicate that above C_6H_{14}, a weak intermolecular correlation appears which approaches a limiting value in the region C_{20}–C_{24}. This view is consistent with the *RDF* data

Table 3 Intermolecular peak positions

Sample	1	2	3	4
Hexane	5.5	10.1	14.7	
Octane	5.5	10.1	14.7	
Hexadecane (20°C)	5.5	10.1	14.7	19.0
Hexadecane (60°C)	5.7	10.4	15.0	
Hexatriacontane (77°C)	5.7	10.3	15.0	19.5
Hexatriacontane (110°C)	5.8	10.6	15.4	20.3
Molten polyethylene (165°C)	5.8	10.6	15.5	
Hexatriacontane (20°C)	4.05, 5.22	9.1, 10.2	12.6, 13.71	16.02 17.82

as an increased *CMO* would have the effect of increasing the number of atoms spaced at distances ~5 Å, and hence increasing the number and amplitude of the intermolecular peaks observed. However, the range of ordering observed is short and no intermolecular correlations are observed beyond r ~20 Å in any of the systems measured. Thus the *RDF* data rule out the existence of parallel arrangements of chain segments over dimensions greater than ~20 Å. Theoretical Monte Carlo[22] simulations of liquid alkanes indicate the possibility of two thermodynamically stable states, one of which contains no molecular correlations, and the other containing configurations with molecular correlations between neighbouring chains. The normal liquid, considered as an average over the two states gives an enhanced molecular optical anisotropy in agreement with the experimental findings. Calculations show that the average dimensions of the chain as measured by their radius of gyration or mean square end-to-end distance remain close to the unperturbed values measured in dilute solutions at the theta temperature. Thus the *RDF* data on liquid alkanes are consistent with a weak correlation of molecular orientation which is a function of chain length, but which does not lead to substantially parallel arrangements of chain segments over large regions (50–100 Å) as suggested previously[23]. Any correlations of molecular orientation are restricted to distances considerably less than 50 Å.

Similarly for molten polyethylene, the *RDF* exhibits less intermolecular ordering than for the higher alkanes (C_{16}–C_{36}). Thus we see that not only does the large increase in molecular weight of the polymer compared with alkane not produce a corresponding increase in order, but that the reduction in freedom of motion (brought about by the increase in melt viscosity, chain entanglements etc.) effectively reduces the degree of molecular interaction occurring as ordering of chain segments. The *RDF* results are therefore consistent with relatively short range correlations over distances less than ~20 Å but which do not increase the average molecular dimensions measured by small-angle neutron scattering[10,11].

REFERENCES

1 'Physical Structure of the Amorphous State', (Eds. G. Allen and S. E. B. Petrie) Marcel Decker, New York, 1976
2 Ovchinnikov, J. K. and Markova, G. S. *Vysokomol Soedin (A)* 1967, **9**, 449
3 Ovchinnikov, J. K., Markova, G. S. and Kargin, V. A. *Polym. Sci. USSR (A)* 1969, **11**, 329
4 Voigt-Martin, I. and Mijlhoff, F. C. *J. Appl. Phys.* 1975, **46**, 1165
5 Longman, G. W., Wignall, G. D. and Sheldon, R. P. *Polymer* 1976, **17**, 485
6 Tancrede, P., Botherell, P., de St Romain, P. and Peterson, D. *J. Chem. Soc. (Faraday Trans. 2)* 1977, **73**, 15
7 Te Lam, V., Picker, P., Patterson, D. and Tancrede, P. *J. Chem.*